Pressure-enhanced dynamic heterogeneity in block copolymers of poly(methyl vinyl ether) and poly(isobutyl vinyl ether)

K. Mpoukouvalas and G. Floudas
University of Ioannina, Department of Physics, P.O. Box 1186, 451 10 Ioannina, Greece
and Foundation for Research and Technology-Hellas (FORTH), Biomedical Research Institute (BRI), Greece

B. Verdonck and F. E. Du Prez
Department of Organic Chemistry, Polymer Chemistry Research Group, Krijgslaan 281 S4, Ghent University, B-9000 Ghent, Belgium
(Received 2 January 2005; published 7 July 2005)

The static structure factor and associated dynamics have been investigated in a series of block copolymers of poly(methyl vinyl ether) (PMVE) and poly(isobutyl vinyl ether) (PiBVE) using x-ray scattering and dielectric spectroscopy (DS). The origin of the dynamic arrest at the glass temperature (T_g) of PiBVE has been explored by temperature- and pressure-dependent DS and pressure-volume-temperature measurements. Both temperature and volume are responsible for the segmental dynamics but temperature has a stronger effect. The copolymers display a minimal dynamic asymmetry ($\Delta T_g \sim 7$ K), nevertheless, are spatially and dynamically heterogeneous. Increasing pressure, unlike temperature, enhances the dynamic heterogeneity. This effect originates from the distinctly different pressure sensitivities of the homopolymers and can be traced back to differences in local packing.

DOI: 10.1103/PhysRevE.72.011802 PACS number(s): 36.20.−r, 64.70.Md, 61.41.+e, 77.84.Nh

I. INTRODUCTION

Dynamic heterogeneity is of key importance in discussing the dynamics of miscible (and immiscible) polymer blends and copolymers [1–6]. In the case of immiscible blends the component dynamics are indistinguishable from the respective homopolymers. In thermodynamically miscible blends, the heterogeneity is again reflected in the presence of segments moving with distinctly different rates ("fast" and "slow"). The temperature (and pressure) dependence of these rates is normally different, giving rise to the failure of time-temperature (and time-pressure) superposition and therefore to thermorheological complexity. Despite the different views on the origin of dynamic heterogeneity in miscible blends (including effects from chain connectivity [1,7,8], local concentration fluctuations [9,10], and inherent differences in the local dynamics of the constituents [11]), there is consensus that the disparity in the glass transition temperatures (T_g) of the homopolymers can enhance the dynamic heterogeneity. Alternatively, in polymer blends with a low T_g contrast ($\Delta T_g < 20$ K), this dynamic heterogeneity is difficult to be resolved experimentally [12].

Recently, pressure-dependent dynamic measurements at and above T_g have been of paramount importance in exploring the origin of the dynamic arrest by lowering T near T_g, in amorphous polymers [13] as well as in polymers possessing orientational order [14]. Pressure can affect the dynamics of miscible and immiscible polymer blends. Recently, ours and other groups have made an effort to investigate the effect of pressure on the dynamic heterogeneity of miscible polymer blends. The effect of pressure was investigated on (i) an athermal diblock copolymer of polyisoprene-*b*-poly(vinyl ethylene) (PI-*b*-PVE) [15], (ii) a miscible (but not athermal) blend of polystyrene/poly(methyl vinyl ether) (PS/PMVE) [13,16], and (iii) in hydrogen-bonded blends of poly(ethyl vinyl ether) (PEVE) [17] and poly(vinyl acetate) (PVA) [18] with poly(4-vinyl phenol) (PVPh). From these systems, by far the strongest effect of pressure was found in the PI-*b*-PVE diblock copolymer, where pressure induced dynamic homogeneity.

For pressure studies, systems of interest include homopolymers with similar structural units and with a small dynamic asymmetry, where temperature alone is not capable of accessing the degree of heterogeneity. The present system is composed of two structurally similar polymers: poly(methyl vinyl ether) (PMVE) and poly(isobutyl vinyl ether) (PiBVE). A series of PMVE-*b*-PiBVE diblock and triblock copolymers was prepared [19] and have been investigated earlier for their remarkable thermoadjustable surfactant properties and for their ability to create colloidal dispersions of organic pigments with stabilities that can be tuned as a function of temperature [19,20]. These thermoresponsive properties originate from the lower critical solution temperature (LCST) behavior of the PMVE segments in an aqueous environment [21]. We have studied the same block copolymers together with PMVE/PiBVE blends using temperature- and pressure-dependent dielectric spectroscopy (DS). The respective homopolymers are closely matched in their glass transition temperatures ($\Delta T_g \sim 7$ K) and can be considered as "dynamically symmetric." However, the application of pressure induces (or better enhances) the existing dynamic heterogeneity. We show that the reason behind this is the distinctly different pressure sensitivities of the two homopolymers. We discuss the role of packing in the dynamic heterogeneity of polymer blends and copolymers.

II. EXPERIMENT

Samples. Both PMVE and PiBVE were prepared as described elsewhere [22]. Figure 1 gives the repeat units of PMVE and PiBVE.

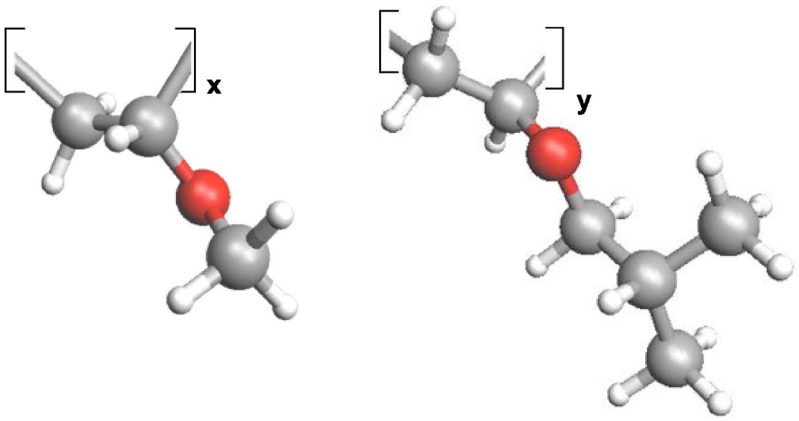

FIG. 1. (Color online) Repeat units of PMVE (left) and PiBVE (right).

The block copolymers were prepared by "living" cationic polymerization using sequential addition of monomers as described elsewhere in detail [19]. Briefly, the polymerizations were carried out with the system acetal/trimethylsilyl iodide as initiator and ZnI_2 as activator. The initiating system based on diethoxyethane leads to *AB* block copolymers whereas the initiating system based on tetramethoxypropane leads to *ABA* or *BAB* triblock copolymers. In this way a series of diblock and triblock copolymers with controlled molecular weights for each segment and narrow polydispersities (between 1.04 and 1.35) has been prepared. Table I gives the molecular characteristics of the systems investigated.

Differential scanning calorimetry (DSC). A Mettler Toledo Star DSC was used. All samples were first heated to 373 K with 10 K/min and subsequently cooled to 200 K with the same rate. The glass temperatures (T_g) were obtained from a second heating run with the same rate. The obtained T_g's of the homopolymers were at 244 K for PMVE (with a width of $\delta T_g \sim 19$ K (obtained from the deviation from the base line) and a heat capacity step of $\delta c_P = 0.53$ J/gK), and 250.5 K for PiBVE ($\delta T_g \sim 20$ K $\delta c_P = 0.38$ J/gK). In all copolymers, a single albeit broader T_g was obtained ($\delta T_g \sim 22$ K, $0.4 < \delta c_P < 0.5$ J/gK), at some intermediate temperatures. The thermograms during the second heating run (10 K/min) for the homopolymers and the $PVME_{38}$-*b*-$PiBVE_{54}$ diblock copolymer are shown in Fig. 2.

TABLE I. Molecular characteristics of the homopolymers and the diblock and triblock copolymers.

Sample[a]	f_{PMVE}
$PMVE_{120}$	1
$PiBVE_{80}$	0
$PMVE_{300}$-*b*-$PiBVE_5$	0.97
$PMVE_{72}$-*b*-$PiBVE_3$	0.93
$PMVE_{65}$-*b*-$PiBVE_{11}$	0.80
$PMVE_{45}$-*b*-$PiBVE_{10}$	0.72
$PMVE_{38}$-*b*-$PiBVE_{54}$	0.29
$PiBVE_{22}$-*b*-$PMVE_{75}$-*b*-$PiBVE_{22}$	0.50
$PiBVE_{34}$-*b*-$PMVE_{45}$-*b*-$PiBVE_{34}$	0.28
$PiBVE_{26}$-*b*-$PMVE_{40}$-*b*-$PiBVE_{26}$	0.31
$PMVE_{62}$-*b*-$PiBVE_{10}$-*b*-$PMVE_{62}$	0.88
$PMVE_{65}$-*b*-$PiBVE_{26}$-*b*-$PMVE_{65}$	0.74
$PMVE_{50}$-*b*-$PiBVE_{20}$-*b*-$PMVE_{50}$	0.74

[a]The number after the abbreviation of each polymer segment indicates the corresponding degree of polymerization.

X-ray scattering. Both wide-angle and small-angle x-ray scattering (WAXS and SAXS) measurements were performed. The WAXS measurements were made with a D8 Advance Bruker diffractometer by using the Cu $K\alpha$ (40 kV, 40 mA) radiation with a secondary beam graphite monochromator. The WAXS patterns were recorded within the 2θ range from 2° to 80° in steps of 0.02° with a counting time of 2 s per step. Figure 3 gives some representative WAXS patterns for the homopolymers and the $PMVE_{38}$-*b*-$PiBVE_{54}$ diblock copolymer at 303 K. SAXS measurements were made using an 18-kW rotating-anode x-ray source with a pinhole collimation and a two-dimensional detector (Siemens) with 1024×1024 pixels. The sample-to-detector distance was 1.5 m. Different measurements of 1 h long were made within the T range $303 < T < 423$ K for the diblock and triblock copolymers.

Pressure-volume-temperature (P-V-T) measurements. Pressure-volume-temperature measurements were made on PiBVE with a fully automated GNOMIX high-pressure dilatometer at the Max-Planck Institute for Polymer Re-

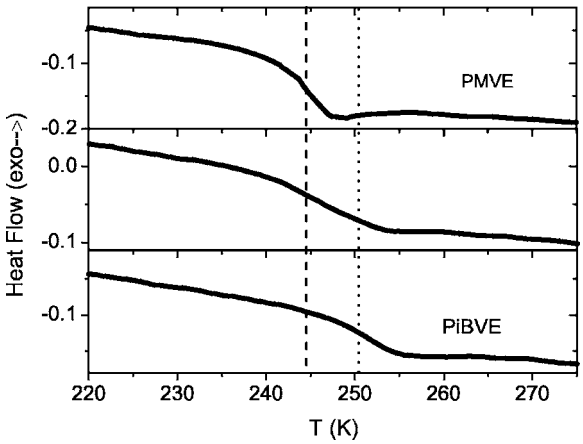

FIG. 2. DSC curves of PMVE (top), PiBVE (bottom), and the $PMVE_{38}$-*b*-$PiBVE_{54}$ diblock copolymer (middle) obtained during the second heating run with 10 K/min. The dashed and dotted vertical lines give the PMVE ($T_g^{DSC} = 244$ K) and PiBVE ($T_g^{DSC} = 250.5$ K) glass temperatures, respectively.

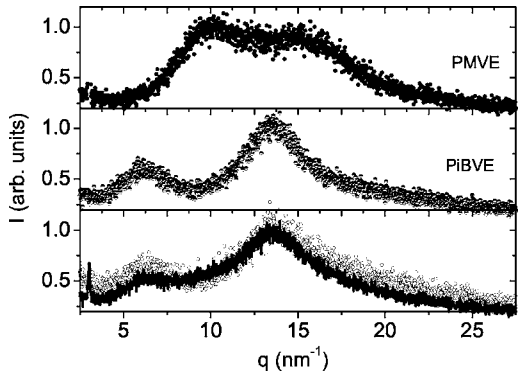

FIG. 3. WAXS curves of PMVE (top), PiBVE (middle), and the diblock copolymer $PMVE_{38}$-*b*-$PiBVE_{54}$ (bottom) at 303 K. In the latter, the symbols are the experimental points and the line is determined from the intensities of the pure components weighted by composition.

search (MPI-P), by A. Best. Both "isothermal" measurements were made within the pressure range from 10 to 200 MPa in steps of 10 MPa and "isobaric" measurements by heating and cooling with a rate of 1 K/min at different pressures. The Tait equation of state was employed:

$$V(P,T) = V(0,T)\left\{1 - 0.0894 \ln\left[1 + \frac{P}{B(T)}\right]\right\}, \qquad (1)$$

where $V(0,T)=1.076+6.3\times10^{-4}T+7.9\times10^{-7}T^2$ (V in cm^3/g, T in °C) is the specific volume at atmospheric pressure and $B(T)=(140\ \text{MPa})\exp(-0.0048\ T)$ (T in °C). For PMVE, literature values were used [23].

Dielectric spectroscopy (DS). The sample cell consisted of two electrodes with 20 mm in diameter and the sample with a thickness of 50 or 20 μm. Both "isobaric" measurements were made at $P=0.1$ MPa by changing temperature in the range from 123 to 453 K and "isothermal" measurements were made at different selected temperatures as a function of pressure and for pressures up to 300 MPa. The frequency range in all cases was in the range from 3×10^{-3} to 1×10^{6} Hz by using a Novocontrol BDS system composed from a frequency response analyzer (Solartron Schlumberger FRA 1260) and a broadband dielectric converter. The complex dielectric permittivity $\varepsilon^*=\varepsilon'-i\varepsilon''$, where ε' is the real and ε'' is the imaginary part, is a function of frequency ω, temperature T, and pressure P, $\varepsilon^*=\varepsilon^*(\omega,T,P)$. In Fig. 4, representative dielectric loss curves are shown for the homopolymers at some selected temperatures. In the analysis of the DS spectra we have used the empirical equation of Havriliak and Negami (HN) [24]:

$$\varepsilon^*(T,P,\omega) = \varepsilon_\infty(T,P) + \frac{\Delta\varepsilon(T,P)}{\{1+[i\omega\tau_{\rm HN}(T,P)]^\alpha\}^\gamma}, \qquad (2)$$

where $\tau_{\rm HN}(T,P)$ is the characteristic relaxation time in this equation, $\Delta\varepsilon(T,P)=\varepsilon_0(T,P)-\varepsilon_\infty(T,P)$ is the relaxation strength of the process under investigation, and α, γ (with limits $0<\alpha$, $\alpha\gamma\leqslant1$) describe, respectively, the symmetrical and asymmetrical broadening of the distribution of relaxation times. In the fitting procedure we have used the ε'' values at

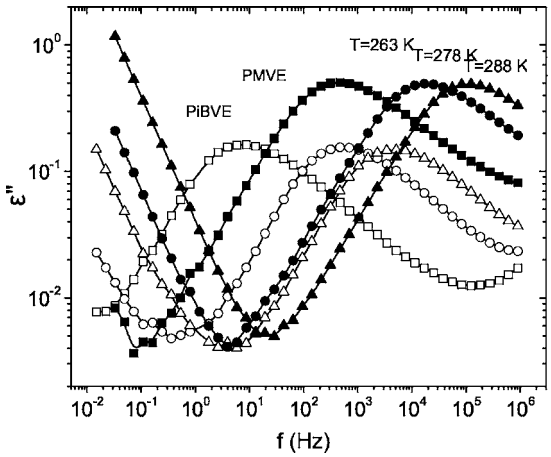

FIG. 4. Dielectric loss curves of PMVE (solid symbols) and PiBVE (open symbols) homopolymers shown at some selected temperatures: (squares) $T=263$ K, (circles) $T=278$ K, and (triangles) $T=288$ K.

every temperature and in some cases the ε' data were also used as a consistency check. The linear rise of the ε'' at lower frequencies is caused by the conductivity which has been included in the fitting procedure as

$$\varepsilon''(T,P,\omega) = \frac{\sigma_{dc}}{\varepsilon_f\omega} - \mathrm{Im}[\varepsilon^*(T,P,\omega)], \qquad (3)$$

where $\sigma_{\rm dc}$ is the dc conductivity and ε_f is the permittivity of free space. From $\tau_{\rm HN}$, the relaxation time at maximum loss, $\tau_{\rm max}$, is obtained analytically following

$$\left[\sin\left(\frac{\pi\alpha}{2+2\gamma}\right)\right]^{1/\alpha}\tau_{\rm max} = \tau_{\rm HN}\left[\sin\left(\frac{\pi\alpha\gamma}{2+2\gamma}\right)\right]^{1/\alpha}. \qquad (4)$$

Alternatively, the modulus representation of the dielectric data can be used through the electric modulus (M^*), related to the dielectric permittivity $\varepsilon^*(\omega)$, through $M^*(T,P,\omega)=1/\varepsilon^*(T,P,\omega)$. The relaxation times obtained from the electric modulus (τ_{M^*}) can differ from the corresponding complex permittivity times (τ_{ε^*}) as $\tau_{M^*}/\tau_{\varepsilon^*}\sim\varepsilon_\infty/\varepsilon_0$, and this difference is exemplified for processes with high dielectric strength. Herein we have employed both representations, but the reported relaxation times are solely from the τ_{M^*} representation.

Apart from the relaxation times, the dipole moment μ of the homopolymers was calculated through the dielectric strength of the segmental process, $\Delta\varepsilon$, as $\Delta\varepsilon=4\pi FNg\mu^2/3k_BT$, where F is the local field correction $[=\varepsilon_0(\varepsilon_\infty+2)^2/3(2\varepsilon_0+\varepsilon_\infty)]$, N is the number of dipoles per unit volume, and g is the Kirkwood-Fröhlich correlation factor of neighboring dipoles. The effective dipole moment $\mu_{\rm eff}=g^{1/2}\mu$ amounts to 1.25 and 0.75 D for PMVE and PiBVE, respectively. The lower value for the latter results from the longer side chain that effectively produce a dilution effect.

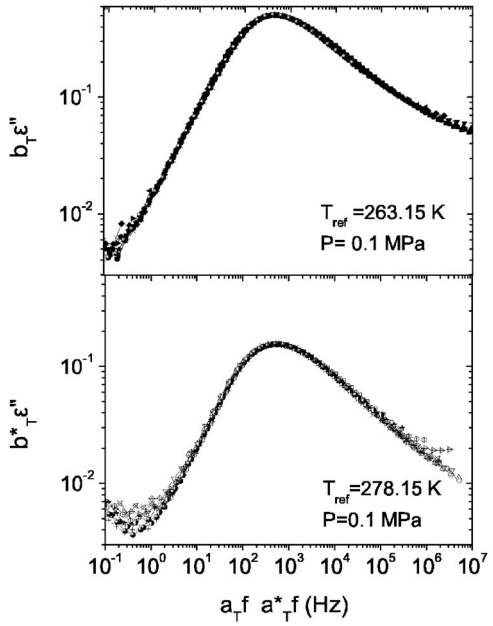

FIG. 5. (Top) Dielectric loss data of PMVE obtained at different temperatures in the range from 248 to 284 K at $P=0.1$ MPa, shifted to the corresponding reference data at $T=263$ K by applying horizontal (a_T) and vertical (b_T) shifts. (Bottom) similar data of PiBVE for different temperatures in the range from 252 to 298 K at $P=0.1$ MPa, shifted to the corresponding reference data at $T=278$ K by applying horizontal (a_T^*) and vertical (b_T^*) shifts.

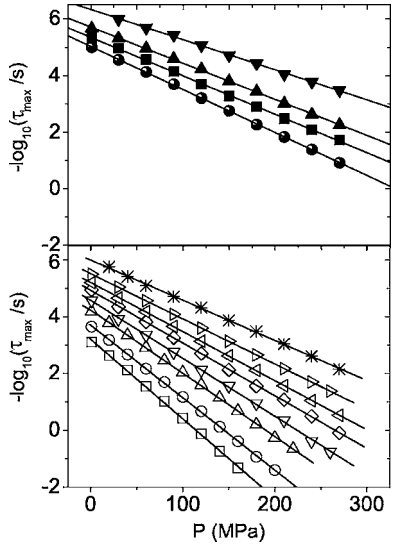

FIG. 6. Relaxation times at maximum loss plotted as a function of pressure for PMVE (top) and PiBVE (bottom) at different temperatures: (●) $T=284$ K, (■) $T=290$ K, (▲) $T=296$ K, and (▼) $T=308$ K for the PMVE and (□) $T=283$ K, (○) $T=288$ K, (△) $T=293$ K, (▽) $T=298$ K, (◇) $T=303$ K, (◁) $T=308$ K, (▷) $T=313$ K, and (∗) $T=323$ K for PiBVE. Notice the stronger $\tau(P)$ dependence for PiBVE.

III. RESULTS AND DISCUSSION

Static structure factor. Amorphous polymers are known to have several broad scattering maxima when examined with wide-angle x-ray (or neutron) scattering with "equivalent" Bragg spacings within the range from 0.1 to 2 nm [25]. The most prominent are (i) the van der Waals (VDW) peak, considered to arise from the VDW contacts of atoms and, (ii) the low van der Waals (LVDW) peak, reflecting mainly interchain correlations. The peak assignment is in general a difficult task, nevertheless T-dependent measurements in several amorphous polymers [polystyrene [26], bis-phenol-A-polycarbonate [27], poly(2-vinylpyridine) [28]] aided in the identification of the LVDW peak from the distinctly different T dependence of the corresponding wave vector (q^*_{LVDW}), below and above the calorimetric T_g. The peak assignment is easier within a homologous series by varying the length of the side chain, as in poly(n-alkyl methacrylates) [29] or in the present system. In Fig. 3, the PMVE and PiBVE homopolymers display distinctly different WAXS patterns with a LVDW peak at $q^*=9.7$ and $q^*=6.3$ nm^{-1}, respectively, reflecting the longer distance between the backbones in the latter due to the longer side chains. In this respect, the two homopolymers differ in their packing efficiency (i.e., have "packing contrast") that is also reflected in their macroscopic densities (1.041 and 0.917 g/cm^3 for PMVE and PiBVE, respectively). In Fig. 3 (bottom), the WAXS curve from the $PMVE_{38}$-*b*-$PiBVE_{54}$ copolymer is also included and can be well reproduced as a weighted sum of the intensities of the individual components (solid line in Fig. 3).

Homopolymer dynamics. The dielectric loss curves for the homopolymers (Fig. 4) are influenced by the main segmental (α) process associated with the glass "transition" and the ionic conductivity at lower frequencies. For the glass "transition" temperature T_g, we use the usual operational definition as the temperature where the segmental relaxation time is at 10^2 s. Faster processes than the α process exist in both homopolymers and the associated relaxation times $\tau(T)$ display Arrhenius T dependences, but their molecular assignment is beyond the scope of the present investigation. Figure 5 shows the result of the time-temperature superposition (tTs) principle for the segmental (α) process in PMVE and PiBVE. The shown "master curves" were obtained by shifting each curve to the maximum loss at a reference temperature by multiplying the frequency axis of each curve by appropriate shift factors (a_T and a_T^* for PMVE and PiBVE, respectively). Small vertical shifts (with corresponding factors b_T and b_T^*) were also necessary. The resulting curves reveal that in both homopolymers the tTs holds (i.e., the distribution of relaxation times does not change with temperature); the shape of the segmental process can be well described by T-independent HN shape parameters $\alpha=0.80\pm0.04$ and $\gamma=0.42\pm0.05$ for both homopolymers.

Despite these similarities the homopolymer segmental processes have distinctly different P dependence as shown in Fig. 6. As expected, pressure slows down the segmental dynamics, but the effect of pressure is stronger for PiBVE.

From the slope of the lines, the apparent activation volume ΔV can be defined as

$$\Delta V = RT\left(\frac{\partial \ln \tau_{\max}}{\partial P}\right)_T \tag{5}$$

originally interpreted as reflecting the difference in molar volume of activated and nonactivated species. Recent experi-

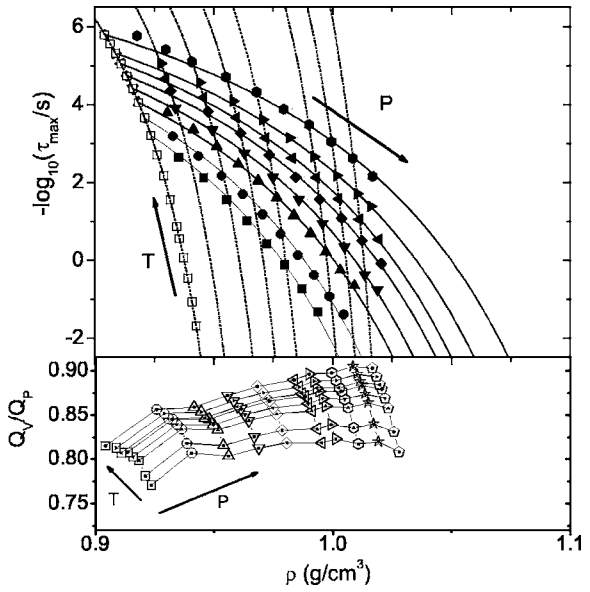

FIG. 7. (Top) "Isothermal" (solid lines) and "isobaric" (dashed lines) relaxation times of PiBVE plotted as a function of density. The isothermal measurements refer to temperatures (■) $T=283$ K, (●) $T=288$ K, (▲) $T=293$ K, (▼) $T=298$ K, (♦) $T=303$ K, (◀) $T=308$ K (▶) $T=313$ K, and (⬢) $T=323$ K. The "isobaric" measurements (open squares) at $P=0.1$ MPa are also shown. (Bottom) Ratio of apparent activation energies under constant volume and pressure conditions, evaluated at the crossings of the "isothermal" and "isobaric" curves, plotted as a function of density.

ments [28,30–32] have shed more light to this quantity: (i) for homopolymers of varying molecular weight it scales with $T-T_g$, (ii) it shows a strong T dependence, increasing by decreasing T, opposite to that of the "free volume," and (iii) it approaches the monomer volume some 70 K above T_g. Recently, ΔV and its T dependence were discussed in terms of the size of cooperative units according to the Adam-Gibbs theory of cooperatively rearranging domains [33]. We will return to the apparent activation volume of the homopolymers later (with respect to Fig. 12).

Of paramount importance in polymer dynamics is the identification of the key parameters that control the segmental dynamics at temperatures near and above T_g [34,35]. According to the simplest "free" volume theory [36], only volume is the control parameter of the dynamics as opposed to different "landscape" models [37] that emphasize the importance of temperature through the associated thermal energy (k_BT). Increasing T affects both the volume (or density) and the thermal energy; therefore, temperature alone cannot separate the two effects. Pressure instead has the advantage that it can be applied under isothermal conditions (affecting solely the density) and provides the means of decoupling the volume and temperature contributions [28,32,35,38]. The relative contribution of volume and temperature in controlling the segmental dynamics can be addressed through the density representation of the relaxation times shown in Fig. 7 for PiBVE.

The "isobaric" and "isothermal" relaxation times can be described by the modified Vogel-Fulcher-Tammann (VFT) equation

$$\tau_{\max} = \tau_0 \exp\left(\frac{D_\rho \rho}{\rho_0 - \rho}\right), \tag{6}$$

where D_ρ is a dimensionless parameter ($D_\rho{}^T=2.75$ and $D_\rho{}^P=1.5$) and ρ_0 is the density at the "ideal" glass state. From the density representation, the ratio of activation energies under constant volume $Q_V=R[\partial \ln \tau_{\max}/\partial(1/T)]_V$ and under constant pressure $Q_P=R[\partial \ln \tau_{\max}/\partial(1/T)]_P$ (or more precisely activation enthalpy) conditions can be obtained directly from the slopes of the "isothermal" and "isobaric" curves as [28]

$$\frac{Q_V}{Q_P} = 1 - \frac{\left(\frac{\partial \ln \tau_{\max}}{\partial \rho}\right)_T}{\left(\frac{\partial \ln \tau_{\max}}{\partial \rho}\right)_P} \tag{7}$$

at their respective crossings. The thus obtained ratio of activation energies is also plotted in Fig. 7 and provides a map of activation energies for the different P, T, and V conditions. This ratio can take values in the range 0–1. A value of zero indicates that volume is the main controlling parameter of the dynamics (i.e., identical relaxation times under isodensity conditions obtained through different T, P paths), whereas a value of one would suggest that thermal energy alone is the controlling parameter. Values in the range 0.7–0.9 are obtained for the different (T, P) conditions for PiBVE. At $T=268$ K ($\sim T_g+18$ K) and $P=0.1$ MPa the ratio of activation energies amounts to ~ 0.73. At the same temperature difference from the respective T_g, this ratio for PMVE amounts to ~ 0.7. In both cases, the segmental dynamics are influenced both by temperature and volume, but between the two it is the former (T) that exerts the strongest influence on the dynamics. This situation for the majority of polymers contrasts with glass-forming liquids with a ratio of ~ 0.5 [39,40] with the exception of liquids with hydrogen bonds [35]. Chain connectivity and the associated intramolecular barriers is one of the factors that control polymer dynamics.

Block copolymer dynamics. All block copolymers investigated are spatially and dynamically heterogeneous and the heterogeneity is exemplified in the more symmetric compositions. As an example we discuss below mainly the $PMVE_{38}$-*b*-$PiBVE_{54}$ diblock copolymer but similar results were obtained for all *AB*, *ABA*, and *BAB* block copolymers of Table I. In Fig. 8, the dielectric loss curve of the $PMVE_{38}$-*b*-$PiBVE_{54}$ diblock copolymer is shown at $T=266$ K and $P=0.1$ MPa. A bimodal distribution is evident, however, with some broadening of the individual loss curves beyond the broadening of the respective homopolymers. The bimodal distribution reflects PMVE- and PiBVE-rich domains large enough to possess individual segmental dynamics (see below with respect to the SAXS results). Surprisingly, this dynamic asymmetry exists despite the minimal difference in the homopolymer glass temperatures ($\Delta T_g \sim 6-7$ K). The sensitivity of the method and the high dielectric activity of both components are the main factors that result in the bimodal distribution as seen by DS. As expected, tTs fails in the copolymers and this is more evident in

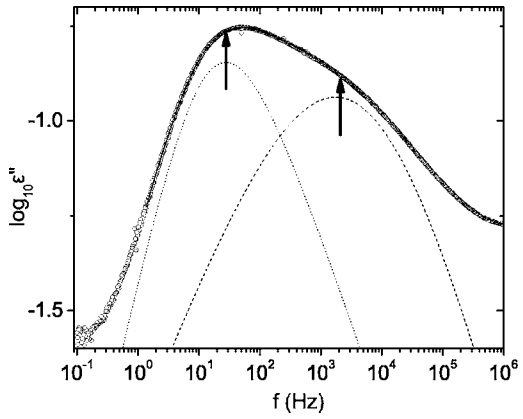

FIG. 8. Detailed dielectric loss curve of $PMVE_{38}$-*b*-$PiBVE_{54}$ diblock copolymer, taken with over 800 frequency points, at $T=266$ K, $P=0.1$ MPa. The dashed ($\Delta\varepsilon=0.6$, $\alpha=0.42$, $\gamma=0.63$, $\tau=5.7\times10^{-4}$ s) and dotted ($\Delta\varepsilon=0.53$, $\alpha=0.73$, $\gamma=0.47$, $\tau=3.6\times10^{-2}$ s) lines give the respective peaks associated with the PMVE and PiBVE components in the copolymer.

the electric modulus representation (not shown here) due to the disparity in the dielectric strengths of the two processes. In all cases, the copolymer segmental dynamics are indistinguishable from the respective homopolymes. This is better shown in Fig. 9 where the $PMVE_{38}$-*b*-$PiBVE_{54}$ segmental dynamics are compared with the PMVE and PiBVE homopolymer dynamics in the usual Arrhenius representation. The solid lines in Fig. 9 are the usual VFT curves for the homopolymers according to

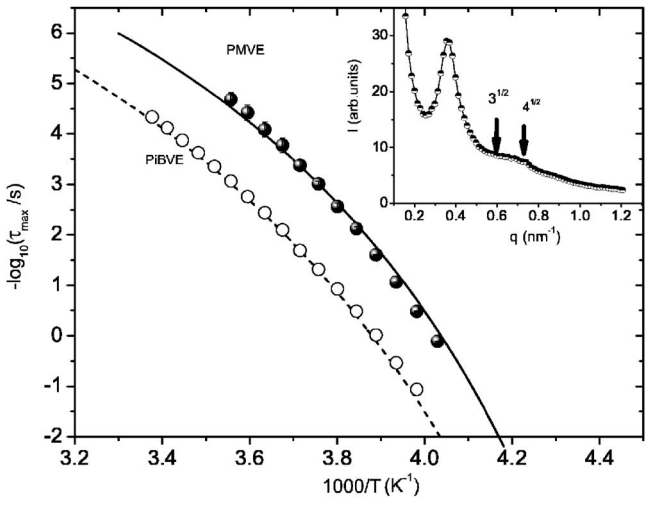

FIG. 9. Relaxation times for the "fast" (solid symbols) and "slow" (open symbols) processes in the $PMVE_{38}$-*b*-$PiBVE_{54}$ diblock copolymer in the usual Arrhenius representation. The solid and dashed lines give the respective VFT dependences of the PMVE and PiBVE homopolymers. In the inset, a small-angle scattering curve from the same copolymer is shown which shows reflections with relative positions with ratios: $1:3^{1/2}:4^{1/2}$ suggesting nanophase separation.

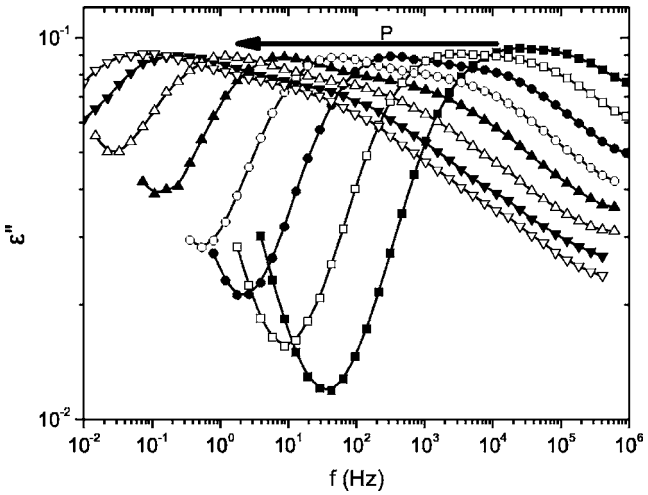

FIG. 10. Dielectric loss curves of the $PMVE_{38}$-*b*-$PiBVE_{54}$ diblock copolymer at $T=290$ K for different pressures: (■) $P=0.1$ MPa, (□) $P=40$ MPa, (●) $P=80$ MPa, (○) $P=120$ MPa, (▲) $P=160$ MPa, (△) $P=200$ MPa, and (▼) $P=240$ MPa. The arrow gives the direction of increasing pressure. Notice that pressure induces dynamic heterogeneity.

$$\tau_{\max}=\tau_0\exp\left(\frac{D_T T_0}{T-T_0}\right), \tag{8}$$

where D_T is a dimensionless parameter and T_0 is the "ideal" glass temperature. These parameters for the homopolymers are $\tau_0=1.2\times10^{-12}$ s, $D_T=7.74$, $T_0=193$ K, and $T_g^{DS}=241$ K for PMVE and $\tau_0=1.1\times10^{-12}$ s, $D_T=10.2$, $T_0=188$ K, and $T_g^{DS}=248$ K for PiBVE. The "fast" and "slow" processes in the copolymers are indistinguishable from the respective homopolymers, suggesting spatial heterogeneity. Notice that this situation here is different than in miscible blends or copolymers. In the latter case, the "fast"-moving species relax with rates comparable to the low-T_g component whereas the "slow"-moving species relax with an average rate—i.e., sensing an average T_g. SAXS has been employed to obtain the nanophase morphologies. The result for $PMVE_{38}$-*b*-$PiBVE_{54}$ is shown as an inset to Fig. 9. The main and higher-order SAXS reflections, with relative positions $1:3^{1/2}:4^{1/2}$, suggest a nanophase morphology composed of PMVE cylinders in a matrix made of PiBVE chains with an intercylinder distance of about 20 nm.

To investigate the effect of the block copolymer interface on the dynamics, a PMVE/PiBVE blend was prepared with identical composition with the $PMVE_{38}$-*b*-$PiBVE_{54}$ copolymer ($\varphi_{PMVE}=0.28$) and studied by DS. As expected, the dielectric loss curves were bimodal reflecting the PMVE and PiBVE dynamics but the intensity of the faster process (PMVE) was higher in the blend at the expense of the slower (PiBVE) process. The higher intensity for the slower process in the copolymer may suggest that the mobility at the interface is controlled by the slower moving species (PiBVE).

The effect of pressure on the heterogeneous copolymer dynamics is to enhance the dynamic asymmetry. This is shown in Fig. 10, where the dielectric loss curves for $PMVE_{38}$-*b*-$PiBVE_{54}$ are examined under "isothermal" condi-

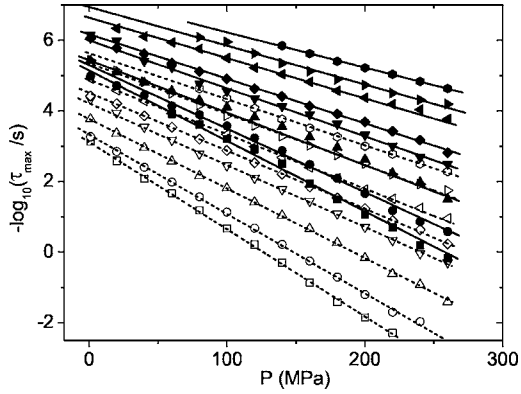

FIG. 11. Pressure dependence of the "fast" (solid symbols) and "slow" (open symbols) processes in the $PMVE_{38}$-*b*-$PiBVE_{54}$ diblock copolymer at different temperatures: (■,□) T=281 K, (●,○) T=284 K, (▲,△) T=290 K, (▼,▽) T=296 K, (♦,◇) T=302 K; (◀,◁) T=308 K, (▶,▷) T=314 K, (⬢) T=320 K. Lines are linear fits to the relaxation times.

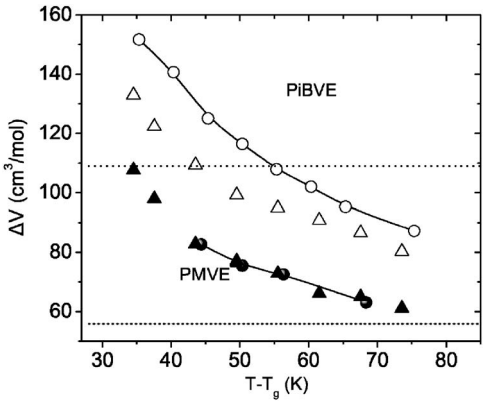

FIG. 12. T_g-scaled apparent activation volume for the PMVE (●) and PiBVE (○) homopolymers and for the "fast" (▲) and "slow" (△) processes in the $PMVE_{38}$-*b*-$PiBVE_{54}$ diblock copolymer. The dashed and dotted lines give the respective monomer volumes.

tions by increasing pressure. This figure clearly depicts the increasing dynamic heterogeneity with increasing pressure. In some cases, it has been argued that increasing pressure has the same effect as decreasing temperature [16]. The present system provides a clear case where this notion is violated. For example, decreasing T could not enhance the dynamic asymmetry of the block segmental dynamics the way that increasing pressure does. As we will see below, the reason behind the pressure-induced dynamic asymmetry is the different packing properties of the two homopolymers. The result from the analysis of the bimodal copolymer distribution with respect to the "isothermal" relaxation times $\tau(P)$ is shown in Fig. 11.

The linear $\log \tau$ vs P dependence is preserved but the dynamic asymmetry is enhanced by increasing P as shown by the different slopes for the "fast"- and "slow"-moving segments reflecting, respectively, the PMVE and PiBVE segments. From the slopes of the respective "isotherms," the apparent activation volume for each component in the copolymer can be extracted and compared with the respective homopolymer. The result of this comparison is shown in Fig. 12. Notice the strong T dependence of ΔV for both homopolymers and that at $T \sim T_g+75$ (T_g+55) this quantity is comparable to the PMVE (PiBVE) monomer volumes. The "fast" and "slow" processes in the copolymer have an apparent activation volume that is very near to the respective homopolymers. Then the enhanced dynamic asymmetry in the copolymers reflects the disparity in the $\tau(P)$ dependencies of PMVE and PiBVE homopolymers. PiBVE, with the longer side chain and a LVDW peak at 6.3 nm^{-1} (with a corresponding interchain distance of ~1 nm), is poorly packed as compared to PMVE (Fig. 3). The less efficient packing makes PiBVE more prone to pressure and explains its higher apparent activation volume.

From the "isothermal" $\tau(P)$ dependences of the homopolymer times (Fig. 6) and the corresponding "isobaric" $\tau(T)$ dependences (not shown here) the pressure-dependent glass temperatures have been extracted by extrapolation to a segmental relaxation time of $\tau=10^2$ s. The thus obtained $T_g(P)$ for the two homopolymers are plotted in Fig. 13 and fitted with the equation [41]

$$T_g(P) = T_g(0)\left(1 + \frac{b}{a}P\right)^{1/b}, \tag{9}$$

where $T_g(0)$ is the glass temperature at ambient pressure (P=0.1 MPa) and b and a are polymer-specific parameters. For PMVE (PiBVE) these parameters are $T_g(0)$=241 K (248 K), b=4.2 (4.0), and a=1715 MPa (1260 MPa). From the initial slopes of these curves we obtain $(dT_g/dP)_{P\to 0}$ values of 0.15 K/MPa and 0.23 K/MPa for PMVE and PIBVE, respectively, suggesting a stronger P dependence for the latter. In the same figure, the $T_g(P)$ dependences of the "fast" and "slow" processes in the $PMVE_{38}$-*b*-$PiBVE_{54}$ copolymer are also shown and display similar dependences with the corresponding PMVE and PiBVE homopolymers [respectively $(dT_g/dP)_{P\to 0}$ of 0.14 and 0.20 K/MPa]. Therefore the enhanced dynamic asymmetry in the copolymers with increasing P reflects the distinctly different homopolymer de-

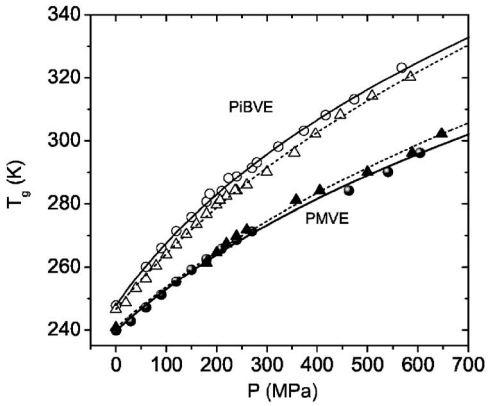

FIG. 13. Pressure dependence of the glass transition temperature of the homopolymers [(●) PMVE, (○) PiBVE] and the "fast" (▲) and "slow" (△) processes in the $PMVE_{38}$-*b*-$PiBVE_{54}$ diblock copolymer. The lines are fits according to Eq. (9).

pendences. For example, from a T_g contrast of only 7 K at 0.1 MPa, a value of 18 K is obtained at 300 MPa which is close to the $\Delta T_g \sim 23$ K for the homopolymers. Thus the homopolymer dynamic asymmetry drives the copolymer component dynamics to become more heterogeneous with the application of pressure. Again, the reason behind the enhanced dynamic asymmetry is a static property—i.e., local packing.

It is of interest now to compare these results for the heterogeneous PMVE-*b*-PiBVE copolymers with other polymer blends and copolymers where both components are dielectrically active. We leave aside the "artificially" compatible PVPh/PVEE [17] and PVPh/EVA [18] blends, where pressure can influence the strength of hydrogen bonds and the phase state. Then the only available system is the athermal PI-*b*-PVE diblock copolymer. In that system, with a ΔT_g of 70 K, the dynamic heterogeneity was reflected in the "fast" and "slow" processes reflecting the relaxation of the low-T_g (PI) and high-T_g (PVE) components. Application of pressure was found to induce dynamic homogeneity—i.e., to similar rates of relaxation for the two components. As in the present case, the reason behind this effect is the different pressure sensitivity of the two components. However, unlike the present case, where $\Delta V_{\text{fast}} < \Delta V_{\text{slow}}$, in PI-*b*-PVE the fast moving species (PI) possess the higher apparent activation volume—i.e., $\Delta V_{\text{fast}} > \Delta V_{\text{slow}}$; thus increasing pressure results in a more dynamically miscible system.

IV. CONCLUSIONS

We have studied (i) the relative contribution of thermal energy and of the available volume in causing the steric constraints responsible for glass formation in PiBVE in comparison to the structurally similar PMVE and (ii) the effect of temperature and pressure on the dynamic heterogeneity in a series of PMVE-*b*-PiBVE diblock copolymers and PMVE/PiBVE blends possessing a minimal dynamic asymmetry ($\Delta T_g \sim 7$ K).

With respect to the PiBVE homopolymer we found that both decreasing temperature and decreasing volume are responsible for the slowing down of the segmental dynamics near T_g. However, between the two, it is temperature that exerts the stronger influence.

With respect to the spatially heterogeneous PMVE-*b*-PiBVE copolymers, we found that pressure, unlike temperature, induces dynamic heterogeneity. The reason for the enhanced dynamic asymmetry is the different pressure sensitivity of the homopolymers. The apparent activation volume of PiBVE is higher than of PMVE, making PiBVE more pressure sensitive. The difference in the apparent activation volumes of the homopolymers could be traced back to the differences in their local packing.

ACKNOWLEDGMENTS

We would like to thank A. Best (MPI-P) for the *P-V-T* measurements on the bulk PiBVE and the XRD unit of the Laboratory Network, at the UoI. We acknowledge G. Tsoumanis (UoI) for technical support. This work was supported by GSRT Grant No. (PENED01/529). F.D.P. acknowledges the ESF project STIPOMAT for financial support.

[1] J. B. Miller, K. J. McGrath, C. M. Roland, C. A. Trask, and A. N. Garroway, Macromolecules **23**, 4543 (1990).
[2] G.-C. Chung and J. A. Kornfield, Macromolecules **27**, 964 (1994).
[3] C. M. Roland and K. L. Ngai, Macromolecules **25**, 363 (1992).
[4] J. A. Pathak, R. H. Colby, G. Floudas, and R. Jerome, Macromolecules **32**, 2553 (1999).
[5] S. Kamath, R. H. Colby, S. K. Kumar, K. Karatasos, G. Floudas, G. Fytas, and J. Roovers, J. Chem. Phys. **111**, 6121 (1999).
[6] S. Kamath, R. H. Colby, and S. K. Kumar, Macromolecules **36**, 8567 (2003).
[7] T. P. Lodge and T. C. B. McLeish, Macromolecules **33**, 5278 (2000).
[8] R. Kant, S. K. Kumar, and R. H. Colby, Macromolecules **36**, 10087 (2003).
[9] A Zetsche and E. W. Fischer, Acta Polym. **45**, 168 (1994).
[10] S. Kumar, R. H. Colby, S. H. Anastasiadis, and G. Fytas, J. Chem. Phys. **105**, 3777 (1996).
[11] A. Arbe, A. Alegria, J. Colmenero, S. Hoffmann, L. Willner, and D. Richter, Macromolecules **32**, 7572 (1999).
[12] J. A. Pathak, R. H. Colby, S. Y. Kamath, S. K. Kumar, and R. Stadler, Macromolecules **31**, 8988 (1998).
[13] G. Floudas, in *Broadband Dielectric Spectroscopy*, edited by F. Kremer and A. Schönhals (Springer, Berlin, 2002), Chap. 8.
[14] G. Floudas, Prog. Polym. Sci. **29**, 1143 (2004).
[15] G. Floudas, G. Fytas, T. Reisinger, and G. Wegner, J. Chem. Phys. **111**, 9129 (1999).
[16] A. Alegria, D. Gomez, and J. Colmenero, Macromolecules **35**, 2030 (2002).
[17] K. Mpoukouvalas, G. Floudas, S. H. Zhang, and J. Runt, Macromolecules **38**, 552 (2005).
[18] S. H. Zhang, R. Casalini, J. Runt, and C. M. Roland, Macromolecules **36**, 9917 (2003).
[19] B. Verdonck, E. Goethals, and F. E. Du Prez, Macromol. Chem. Phys. **204**, 2090 (2003).
[20] N. Bulychev, I. Arutunov, V. Zubov, B. Verdonck, T. Zhang, E. Goethals, and F. Du Prez, Macromol. Chem. Phys. **205**, 2457 (2004).
[21] S. Schäfer, R. Moerkerke, H. Berghmans, R. Koningsveld, K. Dušek, and K. Šolc, Macromolecules **30**, 410 (1997).
[22] W. Reyntjens and E. J. Goethals, Designed Monomers Polym. **4**, 195 (2001).
[23] T. Ougizawa, G. T. Dee, and D. J. Walsh, Macromolecules **24**, 3834 (1991).
[24] S. Havriliak and S. Negami, Polymer **8**, 161 (1967).
[25] R. L. Miller, R. F. Boyer, and J. Heijboer, J. Polym. Sci., Polym. Phys. Ed. **22**, 2021 (1984).
[26] H.-G. Killian and K. Boueke, J. Polym. Sci. **58**, 311 (1962).

[27] G. Floudas, T. Pakula, M. Stamm, and E. W. Fischer, Macromolecules **26**, 1671 (1993).
[28] P. Papadopoulos, D. Peristeraki, G. Floudas, G. Koutalas, and N. Hadjichristidis, Macromolecules **37**, 8116 (2004).
[29] G. Floudas and P. Stepanek, Macromolecules **31**, 6951 (1998).
[30] G. Floudas and T. Reisinger, J. Chem. Phys. **111**, 5201 (1999).
[31] G. Floudas, C. Gravalides, T. Reisinger, and G. Wegner, J. Chem. Phys. **111**, 9847 (1999).
[32] K. Mpoukouvalas and G. Floudas, Phys. Rev. E **68**, 031801 (2003).
[33] C. A. Solunov, J. Phys.: Condens. Matter **14**, 7297 (2002).
[34] M. L. Ferrer, C. Lawrence, B. G. Demirjian, D. Kivelson, C. Alba-Simionesco, and G. Tarjus, J. Chem. Phys. **109**, 8010 (1998).
[35] C. M. Roland, M. Paluch, T. Pakula, and R. Casalini, Philos. Mag. **84**, 1573 (2004).
[36] See, for example, J. D. Ferry, in *Viscoeleastic Properties of Polymers*, 3rd ed. (Wiley, New York, 1980).
[37] C. A. Angell, Science **267**, 1924 (1995).
[38] R. Casalini and C. M. Roland, J. Chem. Phys. **119**, 4052 (2003).
[39] M. Naoki, H. Endou, and K. Matsumoto, J. Phys. Chem. **91**, 4169 (1987).
[40] M. Paluch, C. M. Roland, R. Casalini, G. Meier, and A. Patkowski, J. Chem. Phys. **118**, 4578 (2003).
[41] S. P. Andersson and O. Andersson, Macromolecules **31**, 2999 (1998).